7th International Conference
"New Horizons Towards Sustainable Development"
6-7 November 2023, Dina Al-Maadawi Hotel, Egypt
International Journal of Environmental Studies and Researches (2023), 2 (4):35-51

Active Fieldwork Measurements as Tools for Estimating the Natural Radioactivity at Sadat City, Egypt

Ahmed H.E. Abd El-Mawgoud[1], Magda M. R. Abou El-Safa[1], Sayed F.Hassan[2], Tahra E. Mohammed[2], Ali. H. Saleh[*1]

[1]Survey of Natural Resources in Environmental System Department, Environmental Studies and Research Institute, University of Sadat City, 32897, Sadat City, Egypt.
[2]Nuclear Materials Authority, P.O.Box 530, Maadi, Cairo, Egypt

*Corresponding author : Ali.saleh@esri.usc.edu.eg

Abstract

The present research aims to estimate the concentrations of natural radioactive gamma rays and radon gas in Sadat City's surface and subsurface sediments by using active tools for field measurements. The gamma-dose rate in (µSv/h) directly assessed by using Digilert200 instrument in situ. Whileradon gas (Rn-gas)is estimated in situ by using CR-39. The gamma-ray results range from 0.007 at stations number 25 and 33 to 0.024 at station number 6 and 54, a narrow range was obtained. These values are great far less than the permissible value recommended by the IAEA, 10 (µSv/h). The Rn – gas measures ranged from 0.430±0.351 station no (SI-30) to 4.635±0.930 station no (SA-68). These values are very small compared with the average world values for Rn- gas concentrations ICRP -60. The results of investigated sitesindicate thatthere are no expected potential environmental risks resulting from natural radioactive gamma-rays and Rn-gas in Sadat City surface and sub-surface soil. Add to that, present human activities such as industrial and agricultural have no effects on the radioactive percentage.

Keywords: CR-39, Environmental risks, Gamma rays, Radon gas.

Introduction

The distribution of radionuclides and environmental radiation levels must be understood to evaluate the effects of radiation exposure from terrestrial sources. Natural radionuclides are abundant in the environment of the earth and can be found in a wide range of environmental media, including soil, air, water, rock, plants, sediment, etc., with different quantities depending on the climatic and geological conditions (**Saleh and Shayeb, 2014; Huang et al., 2015; Osman, et al., 2022**). The sources of radiation in our environment are both human activities and geogenic. Anthropogenic sources barely make up any of the overall ambient radioactivity. The different geological formations are primarily responsible for the accumulation and movement of pollutants within a geographic region (**Ramasamy et al., 2014; Abd El-Halim et al., 2017**).Given the radioactive risks to the populace, gamma rays and radon gas are the most significant byproducts of the radioactivity of terrestrial radioisotopes (**UNSCEAR, 2010**). Populations are exposed to gamma rays externally, and the primary sources of their dose are Tl^{-208} and Ac^{-228} of the Th^{-232} disintegration chain, Pb^{-214} and Bi^{-214}, which are generated from R^{-226} of the U^{-238} disintegration chain, and K^{-40}. On the other side, internal exposure is brought on by radon gas, specifically Rn^{-222}, which results from the decay of radium (Ra^{-226} of the U^{-238} chain) (**Aykamis et al., 2013**). Numerous health issues, including acute leukopenia, anaemia, leukaemia, oral necrosis, tooth fracture, cataracts, as well as lung, pancreatic liver, hepatic, bone, and kidney malignancies, could be brought on by long-term radiation exposure and radioactive inhalation (**Qureshi et al., 2014**).

Sadat City is the second new industrial city built in northern Egypt, with an expected estimated population approaching 1,000,000. It was constructed more than four decades ago about 90 km northwest of Cairo on the Cairo–Alexandria Desert Road. Sadat City has a broad industrial base, producing manufactured goods for local and foreign markets. Sadat City was built as a residential, industrial, and agriculture city. Massive and ongoing efforts are being made to develop this area through large-scale agricultural and industrial projects by the government and the public. For that reason, Sadat City was the main area of our study.

The objectives of this study are to observe the distribution of gamma rays in the surface sediment/soil in the investigated area and determine the concentration of Rn-gas in the subsurface sediment of Sadat City using CR-39. Hopefully, the research results will provide baseline information for monitoring radioactive in the Sadat City environment.

Material and Methods

Study area

The study area (Fig. 1) located in the northern of Egypt at 90 Km of Cairo-Alex. Desert Road and covers the hall area of Sadat City. The study area lies between latitudes 30° 17` and 30° 28` N and longitudes 30° 22` and 30° 42` E. Sadat City cover an area of 500 km^2. Four geomorphological units; including conglomerates, sand dunes, old alluvial plains, and young alluvial plains, cover the western Nile Delta region. The arable areas that flank the River Nile's channel and its branches are dominated by young alluvial plains. Irrigation canals and drains cut through these plains, which make up most of the Nile Delta regions. Nearly flat, they slope regionally from south to north and from both sides in the direction of the river channel. Sadat city and its surrounding area belong to the old alluvial plains, which dominate the newly reclaimed lands west of Rosetta branch, with low to moderate elevations ranging from 20 to 60 m asl. The Sadat city is covered by Quaternary clastic composed mainly of sand and gravel with some clay pockets (**Massoud et al., 2014)**. It is a part of the semi-arid zone, which is characterized by a long hot summer and a short warm winter, low rainfall, and high evaporation.

Experimental arrangements

Sample locations selection

There are 70 sites were chosen for measuring the gamma dose rate and Rn-gas concentrations (Fig. 1 and Table 1). The selected sited cover all the area of Sadat City and represent all human activities in the study area as industrial, agricultural, residential and traffic,add to the un-reclaimed areas.

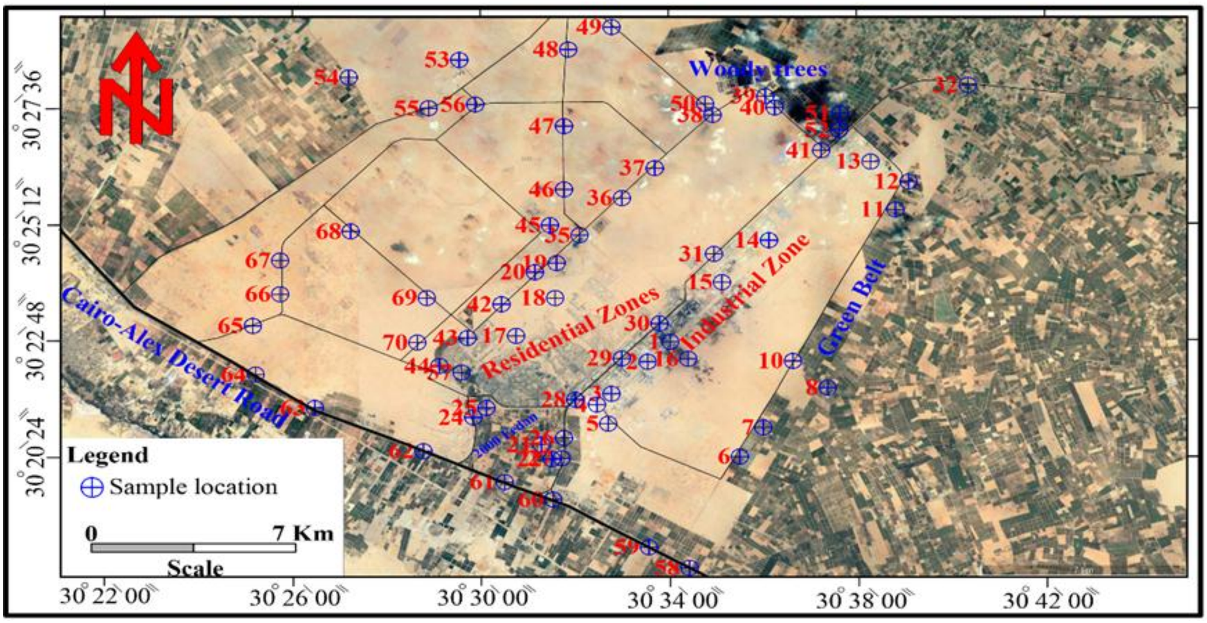

Fig. 1. Landsat map showing the study area and sample locations

Table 1. Description of samples locations.

SN	Symbol	Location		Place
		Latitude N	Longitude E	
1	SI1	30 22.797	30 34.057	Ezz steel
2	SI2	30 22.388	30 33.543	Kima stander
3	SI3	30 21.739	30 32.789	Gheriani Company
4	SI4	30 21.477	30 22.444	Company for Jumpsuits
5	SI5	30 21.153	30 32.673	electricity station
6	SA6	30 20.418	30 35.483	Rizk farm
7	SA7	30 21.024	30 36.003	Safwah farm
8	SA8	30 21.871	30 37.361	The green belt, Damashli manor
9	SA9	30 21.840	30 37.404	The green belt, El Shazly Farm
10	SA10	30 22.373	30 36.649	The green belt, Farm
11	SA11	30 25.531	30 38.825	Northern water station
12	SA12	30 26.096	30 39.079	Alaa's farm
13	SA13	30 26.509	30 38.303	Surface water station
14	SI14	30 24.877	30 36.125	Sphinx Glass Factory
15	SI15	30 24.010	30 35.109	Sphinx Glass Factory behind
16	SI16	30 22.466	30 34.384	An old garbage dump
17	SR17	30 22.928	30 30.735	Environmental Research Institute

Table 1. Cont.

SN	Symbol	Location		Place
		Latitude N	Longitude E	
18	SR18	30 23.721	30 31.583	USC way, Dar Misr Mall
19	SA19	30 24.413	30 31.620	USC farm
20	SI20	30 2.4225	30 31.188	New pond oxidative stress
21	SA21	30 20.678	30 31.320	Ali Khalaf farm
22	SA22	30 20.699	30 31.310	Ali Khalaf farm
23	SA23	30 20.377	30 31.531	Said rizk farm
24	SA24	30 21.236	30 29.839	Esam sabry farm
25	SA25	30 21.418	30 30.142	Sadat City Investors Association
26	SA26	30 20.804	30 31.778	The first Gate of Egypt Road
27	SA27	30 20.376	30 31.720	Mohamed Basuony farm
28	SI28	30 21.594	30 32.017	Ajyal Company
29	SI29	30 22.458	30 33009	Ferchem Egypt for fertilizers
30	SI30	30 23.164	30 33.815	Suez Company
31	SI31	30 24.610	30 34.962	Auto Market Egypt sign
32	ST32	30 28.104	30 40.385	Sadat Road - Kafr Dawood
33	ST33	30 27.948	30 49.153	Gemmayzehbasin ،ramzyatwa
34	SR34	30 27.154	30 49.491	Fahmy Baza school
35	ST35	30 24.975	30 32.118	The intelligent electronic
36	ST36	30 25.794	30 33.010	At the new university wall
37	ST37	30 26.398	30 33.702	After the new university wall
38	ST38	30 27.485	30 34.947	After 5 Km from the new university
39	ST39	30 27.859	30 36.051	After oxidation pondabout 1 Km
40	ST40	30 27.640	30 36.283	After oxidation pondabout 2 Km
41	ST41	30 26.738	30 37.246	After oxidation pondabout 3Km
42	SR42	30 23.581	30 30.461	On the road to the area13 &5
43	SR43	30 22.893	30 29.719	Before the fifth region water tank
44	SR44	30 22.319	30 29.164	Behindthe fifth region
45	SR45	30 25.178	30 31.475	2Km from Right of social housing
46	SR46	30 25.939	30 31.780	5Km from Right of social housing
47	ST47	30 27.255	30 31.802	6Km from Right of social housing
48	ST48	30 28.838	30 31.856	Alongside the western dump tower
49	ST49	30 29.346	30 32.796	After the Gharbia dump tower about 100 m
50	SA50	30 27.702	30 34.808	In front of the old forest gate
51	SA51	30 27.496	30 37.672	In the middle of the old forest gate
52	SA52	30 27.190	30 37.616	In the west of the old forest gate
53	ST53	30 28.613	30 29.526	In front of the wholesale market
54	ST54	30 28.276	30 27.236	After the wholesale market about 2 Km right
55	ST55	30 27.636	30 28.905	The wholesale market road
56	ST56	30 27.701	30 29.903	Olive Road when turning
57	SR57	30 22.177	30 2.9611	In front of Azar fish shop
58	ST58	30 18.154	30 34.406	100m after Al-Khatatba Bridge
59	ST59	30 18.572	30 33.566	After the gate of agriculture company
60	ST60	30 19.551	30 31.519	Before Asole village
61	ST61	30 19.922	30 30.510	2 Km after Asole village
62	ST62	30 20.575	30 2.8777	After gate 2 of Sadat city

Table 1. Cont.

SN	Symbol	Location		Place
		Latitude N	**Longitude E**	
63	ST63	30 21.397	30 26.521	At OPPO sign in desert road
64	ST64	3030 21.8	30 25.242	At 2 Km after OPPO sign in desert road
65	ST65	30 23.157	30 25.150	From Sadat statue to desert road
66	ST66	30 23.798	30 25.768	Intersection of Sadat Road, Alexandria
67	ST67	30 24.447	30 25.770	After 1Km from Intersection of Sadat Road, Alexandria
68	ST68	30 25.100	30 27.250	After 2Km from Intersection of Sadat Road, Alexandria
69	ST69	30 23.714	30 28.871	Ryada University
70	ST70	30 22.767	30 28.654	In the right of Ryada University about 1Km

Gamma dose rate measurement

The gamma exposer dose rate was directly measured at each sample selected cites by Radiation Alert Digilert200 instrument as shown in figure (2).The device features as following:

- Measures alpha, beta, gamma, and X-ray radiation,
- Halogen-quenched Geiger-Mueller tube with mica end window,
- Choose your units: CPM, CPS, µSv/hr, mR/hr, or accumulated counts,
- Audio (can be silenced) and visual signals alert each count,
- Alarm function beeps and flashes when a preset.

Fig. 2. Radiation Alert Digilert 200 Hand held Radiation Detector 81910-04

Measurements of radon gas concentration using CR-39 in the field

The Rn-gas concentrations were measured by using the closed-can techniques (the detectors are sealed so that radon gas only can enter, but not radon daughters 72). This technique is being relatively inexpensive; it provides quite reliable measurements. Thedetector used for measured the concentration of radon gas is the Solid-State Nuclear Track Detectors (SSNTDs) type CR-39. A polymeric form of diethylene glycol (allyl carbonate). Its simple formula is ($C_{12}H_{18}O_7$). CR-39 is very sensitive to ionizing radiation and has the lowest dE/dx threshold of any known SSNTDs. CR-39 (allyldiglycol carbonate) Emin (MeV) ≈ 0.1 and Emax (MeV) > 20.

CR-39 type detector was cut in square shape with dimensions 1x1 cm and mounted in the base of cylindrical plastic cup with height 12 cm and diameter 7 cm. The lid of each cup is punched with a hole, covered with thin piece of filter to allow only for radon gas to enter the cup. The cups were buriedincylindrical hole at depth30-50 cm from the ground surface (Fig 3). The cup with detector left in ground for 130 days "exposure time" from time of hidden to time of collection. After collecting the cups, the detector (CR-39) sheets were removed by using deionized water for two days and then etched using 6.25N NaOH under controlled conditions, constant temperature water bath (70 ±1°C) and time (8hours) (Nabil, 2009). After etching the resulting α-track was counted using optical microscopes at a magnification of 400 X (Model Wolf xsz-107BN Made in China). for each detector, tracks of 50 fields of view were recorded and their average values were used. The radon activity (integrated radon exposure) inside the can was obtained from the track density of the detectors by using the calibration factor 0.242 $Tcm^{-2}d^{-1}/Bqm^{-3}$ obtained from the experiment of calibration by Said et al, 2009.

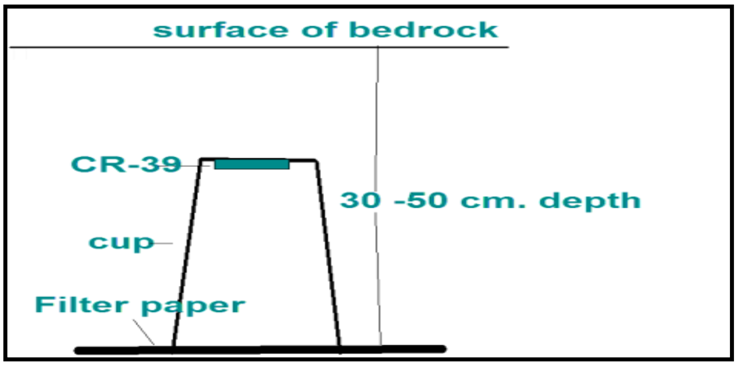

Fig.3. Closed-can techniques configurations.

Etching process

Set the etchant solution to required normality and temperature.A water-bath type GolaboModel VL manufactured in Germany was used to keep the etchant solution at constant temperature to better than ±1°C of the required temperature. The exposed detector put in tube of specific volume of etchant solution in the water bath for the required time. The CR-39 sheets were rinse after complete etching in cold running water for 10-30 min to quickly stop the etching of the left-over etchant in the tracks. After rinsing, wash the samples with distilled water, and dry them with a regular cold hair dryer.

Counting tracks and calculations (CR-39 scanning)

An optical microscope with 400 times magnification was used to count the numberof tracks per field of view; about fifteen fields of view were scanned randomly for each detector. The area of the field of view was calculated by the digital microscope and found to be equal about (0.148 mm^2), the average number of tracks per field of view was used to count the track density per cm^2.

The calculated track density was converted into radon concentrations in Bq/m^3 using the calibration factor (k) obtained by the manufacturer, where every track per cm^2 per day on the CR-39 detectors corresponds to an exposure of 12.3 Bq/m^3 for the activity of radon gas and its daughters. From the measured average track densities (after background subtraction), the radon exhalation rate was calculated via the relation (Sroor, et al, 2001):

$$E = \frac{\rho\lambda v}{\eta A T_{eff}} \qquad (1)$$

Where: E is radon exhalation rate ($Bq\ m^{-2}\ h^{-1}$); ρ is the track density (tracks / cm^2); η is the detector sensitivity ($tracks\ cm^{-2}\ h^{-1}$ / $Bq\ m^{-3}$); λ is the decay constant (= $7.56 \times 10^{-3}\ h^{-1}$); v is the void volume of the container (cm^3); A is the area of the sample (cm^2).

Results and Discussions
Gamma dose rate

The gamma dose rate is used to evaluate the exposure and absorption of radiation to the human body at 1 m above the ground containing naturally occurring radionuclides. The dose rate has been evaluated using the conversion factors (absorbed dose rate in the air per unit activity). Fig. 4 and Table 2 show the spatial distribution of Gama rate in (µSv/h), that directly measured in situ at Sadat City. The measured data recorded lest reading (0.007µSv/h) at station numbers 25 and 33 and highest reading (0.024 µSv/h) at station numbers 6 and 54, a narrow range was obtained. The obtained reading values are great far less than the permissible value recommended by the IAEA (10 µSv/h). The very low concentration read obtained in residential areas can be attributed to the fact that the site is built about forty years ago was a virgin land and very safe for human and there is no potential health risk. The spatial distribution of reading results shows the industrial, agricultural, and traffic activities have significant effect on the Gamma rat reading. So, the concentrations of radionuclides can increase over time, which is need to monitoring program.

Radon gas concentration

Table 3 shows the obtained data for the average track density per field (0.142 mm^2) as well as exposure time per day and station number and location. The exposure time in the field ranged from 109 to 130 day with range of 30 days due to large distance between each station, also the large exposure time may be due to the low values for low experimented gamma dose measured in the field which give an indication for exposure time. Track density/field ranged from 3 to 29, these very small values indicate a very small values for the underground Rn – gas concentrations.

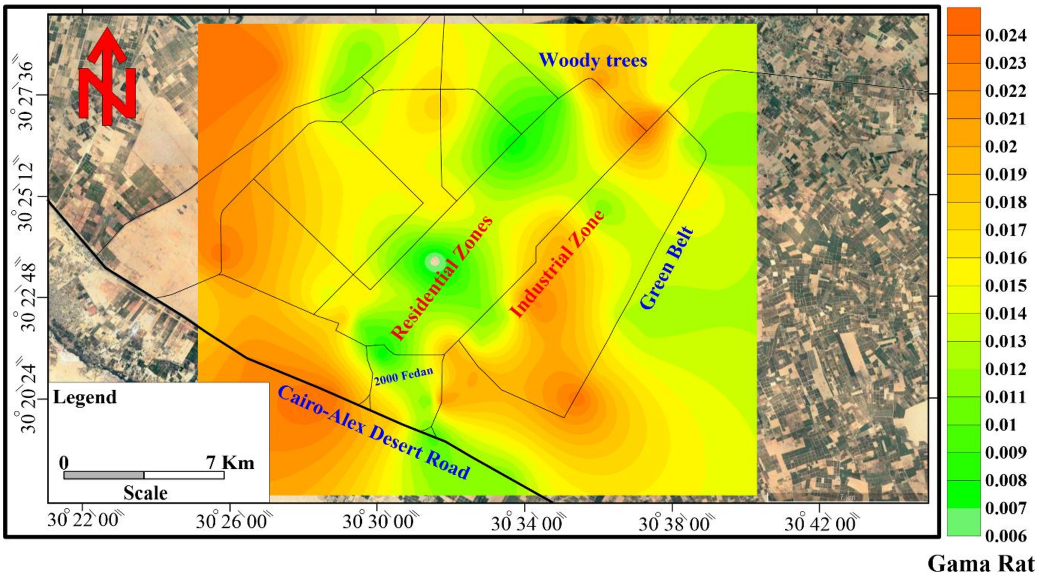

Fig. 4. Spatial distribution of measured gamma dose rat results at Sadat City

Table 2. The results obtained for absorbed dose rate (µSv/h).

SN	Symbol	γ. Rat
1	SI1	0.022
2	SI2	0.013
3	SI3	0.013
4	SI4	0.018
5	SI5	0.020
6	SA6	0.024
7	SA7	0.018
8	SA8	0.013
9	SA9	0.011
10	SA10	0.013
11	SA11	0.016
12	SA12	0.011
13	SA13	0.013
14	SI14	0.011
15	SI15	0.020
16	SI16	0.022
17	SR17	0.013
18	SR18	0.005
19	SA19	0.013
20	SI20	0.011
21	SA21	0.013
22	SA22	0.005
23	SA23	0.011
24	SA24	0.013

Table 2. Cont.

SN	Symbol	γ. Rat
25	SA25	0.007
26	SA26	0.016
27	SA27	0.022
28	SI28	0.020
29	SI29	0.011
30	SI30	0.016
31	SI31	0.018
32	ST32	0.013
33	ST33	0.007
34	SR34	0.011
35	ST35	0.016
36	ST36	0.011
37	ST37	0.007
38	ST38	0.009
39	ST39	0.022
40	ST40	0.018
41	ST41	0.024
42	SR42	0.011
43	SR43	0.016
44	SR44	0.018
45	SR45	0.016
46	SR46	0.014
47	ST47	0.018
48	ST48	0.016
49	ST49	0.014
50	SA50	0.011
51	SA51	0.014
52	SA52	0.022
53	ST53	0.011
54	ST54	0.024
55	ST55	0.011
56	ST56	0.014
57	SR57	0.010
58	ST58	0.014
59	ST59	0.011
60	ST60	0.009
61	ST61	0.018
62	ST62	0.024
63	ST63	0.022
64	ST64	0.018
65	ST65	0.018
66	ST66	0.024
67	ST67	0.022

Table 2. Cont.

SN	Symbol	γ. Rat
68	ST68	0.020
69	ST69	0.016
70	ST70	0.014

Table 3. Average track density per field area as well as exposure time in days.

SN	Symbol	Exposure time (day)	Average track density/field	Average track density/day
1	SI1	133	9	0.068
2	SI2	133	11	0.083
3	SI3	138	12	0.087
4	SI4	138	11	0.080
5	SI5	133	12	0.090
6	SA6	139	14	0.101
7	SA7	139	8	0.058
8	SA8	139	3	0.022
9	SA9	139	4	0.029
10	SA10	139	3	0.022
11	SA11	139	3	0.022
12	SA12	138	5	0.036
13	SA13	137	5	0.036
14	SI14	138	9	0.065
15	SI15	138	5	0.036
16	SI16	137	14	0.102
17	SR17	126	4	0.032
18	SR18	138	3	0.022
19	SA19	138	4	0.029
20	SI20	138	5	0.036
21	SA21	125	5	0.040
22	SA22	125	11	0.088
23	SA23	137	4	0.029
24	SA24	125	10	0.080
25	SA25	125	7	0.056
26	SA26	125	13	0.104
27	SA27	130	9	0.069
28	SI28	130	8	0.062
29	SI29	137	10	0.073
30	SI30	130	2	0.015
31	SI31	137	6	0.044
32	ST32	130	4	0.031
33	ST33	130	3	0.023
34	SR34	130	5	0.038
35	ST35	130	8	0.062

Table 3. Cont.

SN	Symbol	Exposure time (day)	Average track density/field	Average track density/day
36	ST36	130	10	0.077
37	ST37	130	5	0.038
38	ST38	130	11	0.085
39	ST39	130	12	0.092
40	ST40	136	13	0.096
41	ST41	130	16	0.123
42	SR42	116	9	0.078
43	SR43	116	5	0.043
44	SR44	122	10	0.082
45	SR45	116	4	0.034
46	SR46	122	5	0.041
47	ST47	122	12	0.098
48	ST48	122	6	0.049
49	ST49	122	9	0.074
50	SA50	122	8	0.066
51	SA51	109	9	0.083
52	SA52	109	17	0.156
53	ST53	115	3	0.026
54	ST54	115	6	0.052
55	ST55	115	7	0.061
56	ST56	119	6	0.050
57	SR57	115	11	0.096
58	ST58	114	9	0.079
59	ST59	115	8	0.070
60	ST60	114	12	0.105
61	ST61	113	11	0.097
62	ST62	113	21	0.186
63	ST63	113	18	0.159
64	ST64	113	16	0.142
65	ST65	113	12	0.106
66	ST66	120	22	0.183
67	ST67	113	24	0.212
68	ST68	120	20	0.167
69	ST69	120	18	0.150
70	ST70	120	10	0.083

Track density (track/cm^2/day)

Table 4 represents the data for track density (track /Cm^2/ day) using data of Table 3 after divided it by a calibration factor 0f 0.0218 and exposure time. the data shows that, it ranges from 0.007±0.022 station no SA-10 to 0.033±0.167 station no ST-68, the great value for the standard deviation indicates non- uniformity of track density as well as very far low values Rn- gas concentration as will be shown latter.

Table 4. Track/cm^2/day, as well as Radon gas concentration (Bq/m^3).

SN	Symbol	Track/cm^2/ d ± St.V	Rn(Bq/m^3) ±St.V
1	SI1	0.030±0.068	1.889± 0.840
2	SI2	0.023±0.083	2.309± 0.630
3	SI3	0.022±0.087	2.428± 0.607
4	SI4	0.014±0.080	2.226± 0.405
5	SI5	0.015±0.090	2.519± 0.420
6	SA6	0.029±0.101	2.812± 0.803
7	SA7	0.072±0.058	1.607± 2.009
8	SA8	0.014± 0.022	0.602± 0.402
9	SA9	0.014± 0.029	0.803± 0.402
10	SA10	0.007± 0.022	0.603± 0.201
11	SA11	0.007± 0.022	0.603± 0.201
12	SA12	0.014± 0.036	1.012± 0.405
13	SA13	0.015± 0.036	1.019± 0.408
14	SI14	0.014± 0.065	1.820± 0.408
15	SI15	0.014± 0.036	1.012± 0.405
16	SI16	0.022± 0.102	2.853± 0.611
17	SR17	0.016± 0.032	0.886± 0.443
18	SR18	0.007± 0.022	0.607± 0.202
19	SA19	0.014± 0.029	0.809± 0.405
20	SI20	0.014± 0.036	1.012± 0.405
21	SA21	0.016± 0.040	1.117± 0.447
22	SA22	0.022± 0.088	2.457± 0.611
23	SA23	0.016± 0.029	0.815± 0.447
24	SA24	0.024± 0.080	2.234± 0.670
25	SA25	0.024± 0.056	1.564± 0.670
26	SA26	0.024± 0.104	2.904± 0.670
27	SA27	0.023± 0.069	1.933± 0.644
28	SI28	0.023± 0.062	1.718± 0.644
29	SI29	0.022± 0.073	2.038± 0.611
30	SI30	0.008± 0.015	0.430± 0.351
31	SI31	0.015± 0.044	1.223± 0.408
32	ST32	0.015± 0.031	0.859± 0.408
33	ST33	0.008± 0.023	0.644± 0.351
34	SR34	0.015± 0.038	1.074± 0.430
35	ST35	0.015± 0.062	1.718± 0.430
36	ST36	0.023± 0.077	2.148± 0.644
37	ST37	0.015± 0.038	1.074± 0.430
38	ST38	0.015± 0.085	2.363± 0.430
39	ST39	0.023± 0.092	2.577± 0.644
40	ST40	0.022± 0.096	2.669± 0.616

Table 4. Cont.

SN	Symbol	Track/cm^2/ d ± St.V	Rn(Bq/m^3) ±St.V
41	ST41	0.015± 0.123	3.436± 0.430
42	SR42	0.086± 0.078	2.166± 2.400
43	SR43	0.017± 0.043	1.203± 0.481
44	SR44	0.027± 0.082	2.289± 0.749
45	SR45	0.017± 0.034	0.963± 0.481
46	SR46	0.016± 0.041	1.144± 0.458
47	ST47	0.022± 0.098	2.746± 0.687
48	ST48	0.016± 0.049	1.373± 0.458
49	ST49	0.025± 0.074	2.060± 0.687
50	SA50	0.016± 0.066	1.831± 0.458
51	SA51	0.018± 0.083	2.305± 0.512
52	SA52	0.018± 0.156	4.355± 0.512
53	ST53	0.017± 0.026	0.728± 0.486
54	ST54	0.017± 0.052	1.457± 0.486
55	ST55	0.017± 0.061	1.699± 0.486
56	ST56	0.017± 0.050	1.408± 0.469
57	SR57	0.017± 0.096	2.671± 0.69
58	ST58	0.026± 0.079	2.204± 0.735
59	ST59	0.017± 0.070	1.942± 0.486
60	ST60	0.026± 0.105	2.938± 0.735
61	ST61	0.018± 0.097	2.717± 0.494
62	ST62	0.018± 0.186	5.054± 0.494
63	ST63	0.027± 0.159	4.448± 0.741
64	ST64	0.018± 0.142	3.953± 0.494
65	ST65	0.018± 0.106	2.965± 0.494
66	ST66	0.042± 0.183	5.119± 1.163
67	ST67	0.018± 0.212	5.930± 0.494
68	ST68	0.033± 0.167	4.653± 0.930
69	ST69	0.025± 0.150	4.188± 0.698
70	ST70	0.017± 0.083	2.327± 0.465

Radon gas concentration (Bq/m^3)

Table 4 represents the measured Rn- gas concentrations (Bq/m3) in all stations using closed cuptechnique and calculated using equation (2.18) and data for track density presented in table (4) and calibration factor 0f 0.0218 (track /Cm^2/ day). The Rn – gas concentration ranged from 0.430±0.351 station no SI-30 to 4.635±0.930 station no SA-68, these values are very small compared with the average world values for Rn- gas concentrations ICRP -60.

The Rn- gas concentration mainly depends on U- concentration in the underground, porosity and permeability of the bed rock, water content and finally the environmental conditions (temperature, pressure difference, relative humidity, air speed, and the detector response.

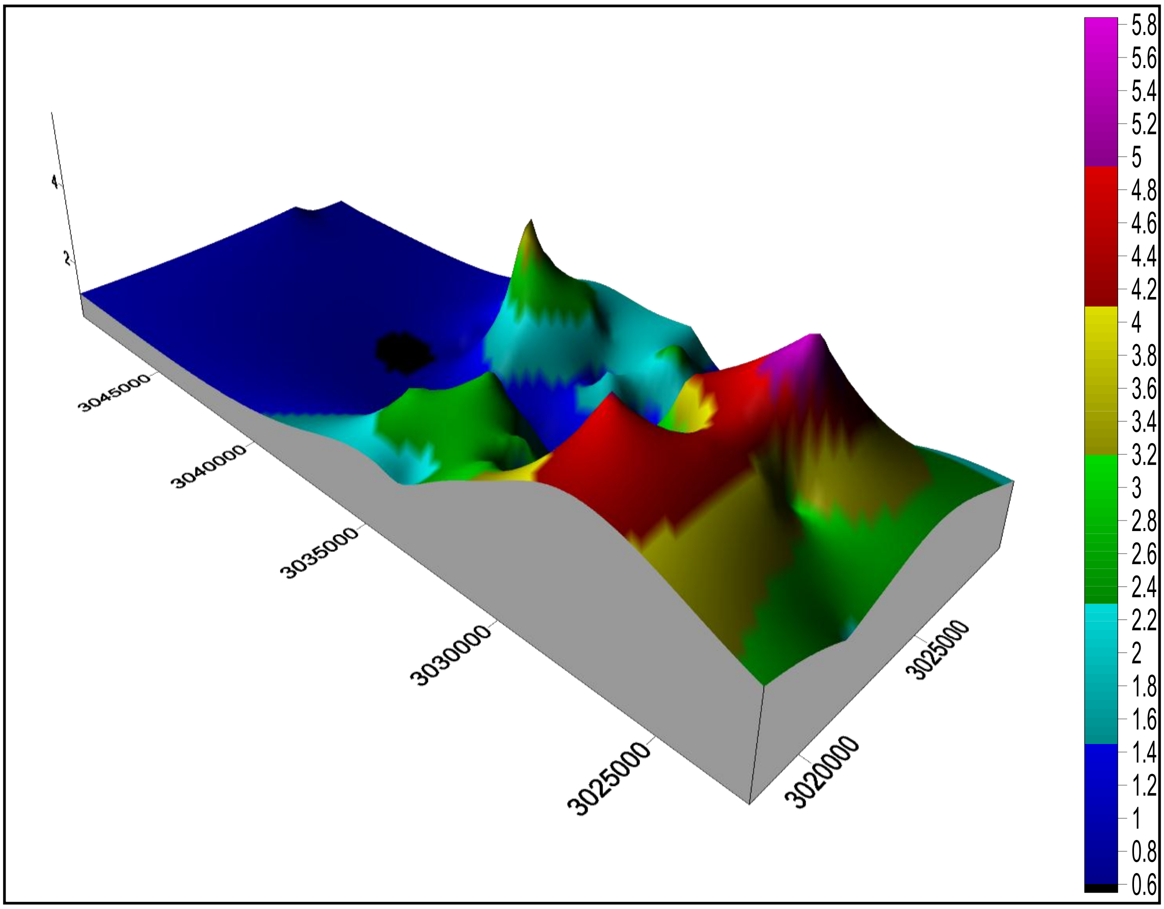

Fig. 5. 3D graphical distribution of Rn- gas concentration in Sadat City

The data in Table 4 for the Rn- gas concentration was graphically represented in surfer map Fig. 5. The figure shows a complete difference in shape compared with that for gamma absorbed dose rate in Fig. 4, stats the true, that gamma radiation comes from different all naturally occurring nuclei not only from the radon as a daughter nucleus of ^{238}U.

Fig. 6 represents graphically the data obtained in Table 4. It can be shown that a fluctuate behavior ranges from maximum to minimum values with relatively high values at the end of the figure.

Conclusion

The concentrations and spatial distribution of natural radioactive gamma rays and radon gas in Sadat City's surface and subsurface sediments were assessed by using active tools for field measurements. The gamma-dose rate in (μSv/h) directly assessed by using Digilert200 instrument in situ. While radon gas (Rn-gas) was estimated in situ by applying the low-cost technique anddelivering quite reliable measurements as closed-can techniques.The Solid-State Nuclear Track Detectors (SSNTDs) type CR-39 is used in the detection of Rn-gas. The gamma rat dose recorded lest reading (0.007 μSv/h) at station numbers 25 and 33 and highest reading (0.024 μSv/h) at station numbers 6 and 54. The obtained reading values are great far less than the permissible value recommended by the IAEA (10 μSv/h).The Rn–gas concentration (Bq/m^3) ranged from 0.430 ± 0.351 at SI-30 to 4.635 ± 0.930 at SA-68, these values are very small compared with the average world values for Rn- gas concentrations ICRP (60Bq/m^3). The very low concentration recorded at residential areas can be attributed to being very safe for human and there is no potential health risk. The spatial distribution of reading results shows the industrial, agricultural, and traffic activities have significant effect on the Gamma rat reading and Rn-gas, which is need to monitoring program.

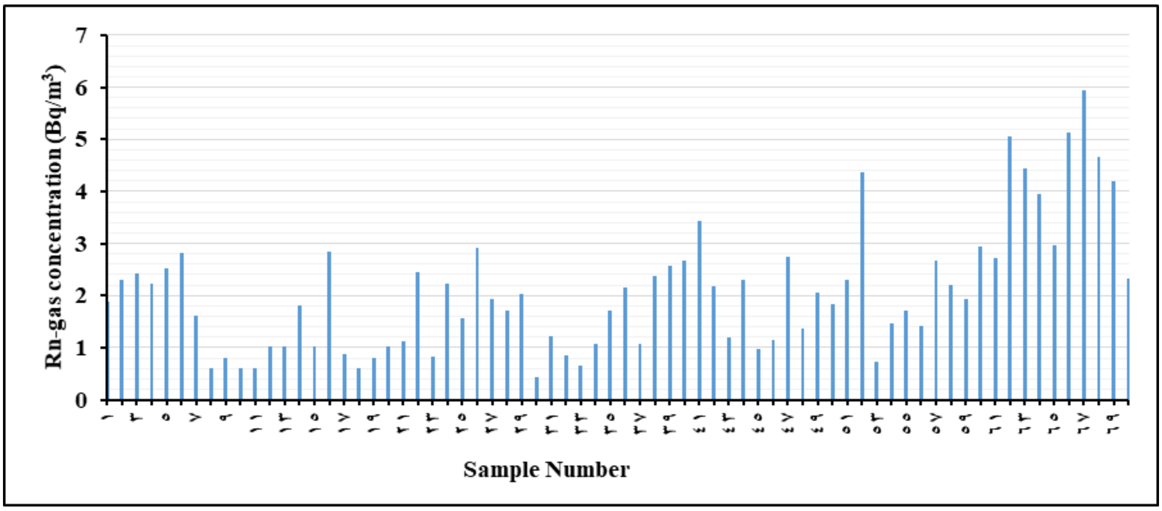

Fig. 6. Histogram for the activity concentration of radon in Sadat City

References

Abd El-Halim, E.S., Sroor, A., El-Bahi, S.M., Ibrahim E.E., Sheikh, E.M.E., Musa K.M. 2017. Assessment of radioactivity levels and hazards for some sedimentary rock samples in different localities southwestern, Sinai, Egypt. International Journal of Recent Scientific Research, 8 (11), 21916 -21922. http://dx.doi.org/10.24327/ijrsr.2017.0811.1164

Agnieszka D_zaluk, Dariusz Malczewski, Jerzy Z_ aba, Maria Dziurowicz. 2018. "Natural radioactivity in granites and gneisses of the Opava Mountains (Poland): a comparison between laboratory and in situ measurements", Journal of Radioanalytical and Nuclear Chemistry 316:101–109.

Annunziata M. F. 2007. Radioactivity Introduction and History. 1st edition: USA, Elsevier,10-132.

ATSDR, T. 2000. ATSDR (Agency for toxic substances and disease registry). Prepared by clement international corp., under contract, 205, 88-0608.

Awad A. Ibraheem, Atef El-Taher, May H. M. A. 2018. Assessment of natural radioactivity levels and radiation hazard indices for soil samples from Abha, Saudi Arabia. Results in Physics 11, 325– 330.

Aykamıs, A. ¸S.; Turhan, ¸S.; Aysun Ugur, F.; Baykan, U.N.; Kılıç, A.M. 2013. Natural radioactivity, radon exhalation rates and indoor radon concentration of some granite samples used as construction material in Turkey. Radiat. Prot. Dosim.157, 105–111. http://doi.org/10.1093/rpd/nct110

Baum, E. M., Knox, H. D., & Miller, T. R. 2002. Nuclides and isotopes: chart of the nuclides. Schenectady, NY: KAPL.

Cohen B. L., 1971. Concepts of Nuclear Physics, New Delhi: Tata MC GrawHill Publishing Company LTD.

Curie, P.1967. radioactive substances, especially radium, Nobel Lecture on June 6, 1905. In: Nobel Lectures in Physics, Amsterdam: Elsevier, 1901–1970.

Das A., Ferbel T.2003. Introduction to Nuclear and Particle Physics. 2nd edition, London: World Scientific Pub. Co., 42-100.

Ehman W., Vance D. E. 1993. Radiochemistry and nuclear methods of analysis. United Kingdom: John Wisely and sons, 51-203.

Eisenbud M., Gesell T.1997. Environmental Radioactivity", 4th edition, UK: Academic Press, 10-85.

Friedlander G., Kennedy J, Miller J.1981. Nuclear and Radiochemistry, 2nd edition, New York: John Wiley and Sons, INC., 54-243.

Huang, Y., Lu, X., Ding, X., Feng, T. 2015. Natural radioactivity level in beach sand along the coast of Xiamen Island, China. Marine Pollution Bulletin 91, 357–361. http://dx.doi.org/10.1016/j.marpolbul.2014.11.046

Krane K. S.1988. Introduction to Nuclear Physics, 3rd edition, New York: Wiley, 160-374.

Leroy C., Rancoita P. G.2004. Principles of Radiation Interaction with Mater and Detection, Singapore: World scientific Pub. Co.

Magill J., Galy J.2005. Radioactivity Radionuclides Radiation, Germany: Springer- Velag, 40-86.

Massoud, U., Kenawy, A.A., Ragab, E.A., Abbas, A.M., El-Kosery, H.M. 2014. Characterization of the groundwater aquifers at El Sadat City by joint inversion of VES and TEM data, NRIAG Journal of Astronomy and Geophysics, 3:2, 137-149, https://doi.org/10.1016/j.nrjag.2014.10.001

Mittal V.K., Verma R.C., Gupta S.C. 2009. Introduction to Nuclear and Particle Physics", New Delhi, 76-141.

Osman, R., Dawood, Y.H., Melegy, A., El-Bady, M.S., Saleh, A.; Gad, A. 2022. Distributions and Risk Assessment of the Natural Radionuclides in the Soil of Shoubra El Kheima, South Nile Delta, Egypt. Atmosphere, 13, 98. https://doi.org/10.3390/atmos13010098

Patel, S.B.1991. Nuclear Physics an Introductory", 1st edition, New Delhi: Daryaganj, 59-92.

Qureshi, A.A., Tariq, Sh., Ud D.K., Manzoor, Sh., Calligaris, Ch., Waheed, A. 2014. Evaluation of excessive lifetime cancer risk due to natural radioactivity in the rivers sediments of Northern Pakistan. Journal of Radiation Research and Applied Sciences, 7, 438-447. https://doi.org/10.1016/j.jrras.2014.07.008

Ralph, E. L., Howard, L. A. 1972. Nuclear Radiation Physics", 4th edition N.J., Englewood Cliffs, 120-280.

Ramasamy, V., Paramasivan, K., Suresh, G. and Jose, M.T. 2014. Role of sediment characteristics on natural level of the Vaigai river sediment, Tamilnadu, India. J. Environ. Radioact. 127, 64-74.

Saleh, H., Shayeb, M.A. 2014. Natural radioactivity distribution of southern part of Jordan (Ma'an) soil. Ann. Nucl. Energy 65, 184–189. https://doi.org/10.1016/j.anucene.2013.10.042

United Nations Scientific Committee on the Effect of Atomic Radiation (UNSCEAR). 2000. Sources and Effects of Ionizing Radiation. Volume I, Annex B. Exposure from Natural Radiation. Report to General Assembly, United Nations, New York.

United Nations Scientific Committee on the Effect of Atomic Radiation (UNSCEAR). 2008. Effects of ionizing Radiation, report to the General Assembly, Vol.1, New York: UN.

UNSCEAR. Sources and Effects of Ionizing Radiation, United Nations Scientific Committee on the Effects of Atomic Radiation (UNSCEAR). 2010. Report; United Nations: New York, NY, USA, Volume I. http://doi.org/10.18356/cb7b6e26-en